

SYNTHESIZED AGRICULTURAL WASTE BASED ADSORBENT COLOCASIAESCULENTA FOR THE REMOVAL TOXIC CHROMIUM (VI): EXPERIMENTAL AND ANALYSIS

¹Soibam Sangeeta and ^{2*}Potsangbam Albino Kumar
^{1,2}National Institute of Technology, Manipur

ABSTRACT

A low-cost abundantly available agricultural product, Colocasia Esculenta was chemically activated and used for the removal of chromium ions from aqueous solutions. The activated carbon was characterized using Scanning Electron Microscope (SEM), Energy Dispersive X-ray Analysis (EDAX) and Brunauer – Emmett – Teller to study the structure, morphology and pore size distributions. Analysis were done using Intra – particle diffusion, pseudo first order and second order kinetic models and Langmuir and Freundlich isotherm models to calculate the adsorption capacities of chromium ions on the adsorbent surface. At pH 2, the adsorbent have a optimum removal percentage of 85.27% Cr (VI) ions after 2 hours. The maximum Cr (VI) adsorption capacity obtained was 5.419 mg/g. From the findings, it can be observed that the pseudo-second-order model best describes the adsorption process. Freundlich isotherm model is more favourable with high correlation coefficient of 0.99. The results demonstrated potential application of AGT for removal of chromium ions from aqueous solutions.

Keywords: Colocasia Esculenta, Chromium ions, Kinetics, Isotherms, Thermodynamics

I. INTRODUCTION

Chromium is the sixth most abundant transition metal constituting about 0.3 mg/kg of the Earth's crust. It is lustrous, hard, and brittle metal. They mainly occur in two oxidation states, out of which Cr (III) and Cr (VI) are most stable [1]. The excess chromium ions present in water causes various health problems because of their carcinogenicity, mutagenicity, genotoxicity, and bioaccumulation. Human exposure to toxic chromium ions has also increased tremendously due to vast industrial and technological applications. The most prominent sources of toxic chromium include mining, smelting, tanning industries, plating, and other industrial operations [2].

Several conventional techniques have been employed for the removal of chromium ions. Some of them are membrane separation, electrocoagulation, reverse osmosis, electrodialysis, flocculation and chelation, ultrafiltration, chemical precipitation, ion exchange and, adsorption [3]. All these technologies have their own merits and demerits. Although

chemical precipitation is the most traditionally used method, it has a disadvantage due to the production of voluminous toxic sludge and incomplete removal, thus suffering from drawbacks. Other techniques require high operating costs, sludge formation, and elaborate pre-treatment requirements for membrane process and disposal problems [4]. The most commonly used process today for heavy metal is the adsorption process. In adsorption, the used of activated carbon for chromium removal, though widely applied is not preferable due to high costs and generation of spent carbon. Synthesis of polymers as adsorbents for the chromium removal is also an area of research in the recent years. Although the use of polymers has a high removal efficiency, the complex process to synthesise the polymer and high cost of operations limits its applications. Due to these economic drawbacks, focus has been shifted for the utilization of cheaper and abundantly available materials like saw dust, rice husk, banana peels, coir pith etc [5]. Hence, adsorption method using agricultural waste based adsorbents can be considered a better alternative for chromium ions removal.

Hence, the present study focuses on the development of novel material with low cost, non – conventional, easily and abundantly available Colocasia Esculenta (Giant Taro) for the detoxification of chromium. Giant taro was chemically modified for effective removal of hexavalent chromium in batch mode operations. The interaction of the adsorbent and chromium metal ions was studied under various pH conditions, Cr (VI) ions concentration, adsorbent dose, adsorption rate, and temperature variations. The studies were conducted on synthetic water and analysis were done using kinetics and isotherm models alongwith thermodynamic studies.

II. MATERIALS AND METHODS

A. Adsorbent and adsorbate preparation

Giant tarowere procured from local market, cut to pieces, washed and sundried. The dried peels were crushed, sieved and treated with phosphoric acid (H_3PO_4). The chemically treated powder was activated and carbonized in the muffle furnace for 30 min at 200°C to remove the non – carbon elements in gaseous forms. The carbonized and Activated Giant Taro(AGT) were stored in the desiccators for further use.

Analytical grade Potassium dichromate ($K_2Cr_2O_7$), ortho phosphoric acid (H_3PO_4), Sodium hydroxide (NaOH),

Sulphuric acid (H₂SO₄), Acetone (CH₃)₂CO, 1,5 Diphenyl-Carbazide and Hydrochloric acid (HCl) 35 % were purchased from Merck specialities private Ltd., India. Sources of chromium ions were prepared from potassium dichromate salt purchased from Merck, India. Initial concentration of chromium standard solution was 1000 mg/L. Lower concentrations for the calibration were obtained from series dilution of the prepared standard solution using dilution factor of 10.

B. Batch Experiment

Batch mode adsorption experiment were conducted at room temperature except where mentioned. All batch studies were carried out with 500mL metal solution in 1L beaker to prevent the spill off of the solution during experiment. Predetermined quantities of adsorbent were added in the beaker and stirred at 250 rpm on the Jar test apparatus. The pH of the solutions were adjusted by using 0.1 N of H₂SO₄ and NaOH. Acid/base were preferred than buffer as it was observed more economical when adsorption experiments were conducted in large scale. The filtrates were separated using Whatman filter paper No. 42 and used for the estimation of the ions. The amount of chromium adsorbed on the adsorbent ABG and the percentage of removal were calculated by:

$$q_t = \frac{C_o - C_t}{m} V \dots \dots \dots (1)$$

$$\% \text{ Removal} = \frac{C_o - C_t}{C_o} \times 100 \dots \dots \dots (2)$$

Where, C_o is the initial concentration (mg/L), C_t is the final concentration (mg/L), m is the mass of the adsorbent (g) and V is the volume of the solution (L).

III. RESULTS AND DISCUSSIONS

A. Adsorbent Characterization

To understand the morphological studies, the surface, textures and pores, scanning electron microscope (SEM) analysis was conducted in 20 micron sizes and 2.00 KV magnifications for the adsorbent AGT as shown in Fig. 1. The SEM image before the adsorption demonstrates the surfaces heterogeneity and presence of multi pores thereby enhancing the metal uptake. The images after the adsorption in Fig. 2 shows a systematic decrease in the porosity with increasing metal concentration. Energy dispersive X-ray diffraction analysis (EDAX) was also investigated Figs. 3 and 4. The EDAX image before and after the adsorption shows the elemental composition and, homogeneity of the structures. During the analysis, different areas were focussed and the corresponding peaks are shown in the images along with the atomic % of the elements present. Thus, confirming the uptake of chromium ions after the adsorption process. Brunauer – Emmett – Teller (BET) analysis were also done to find the specific surface areas and porosity of AGT. It has a surface area of 17.52 m²/g, pore size of 4.231nm and pore volume of 0.19 cm³/g..

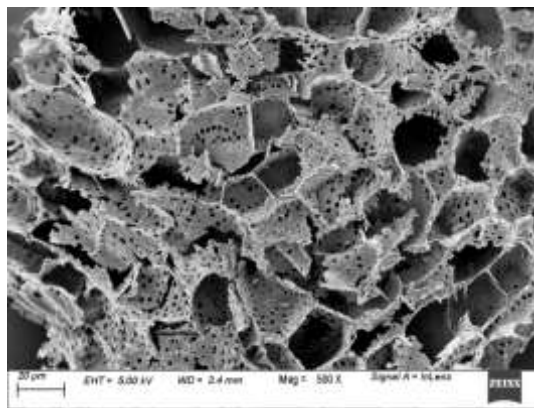


Fig. 1: SEM image of AGT before chromium adsorption

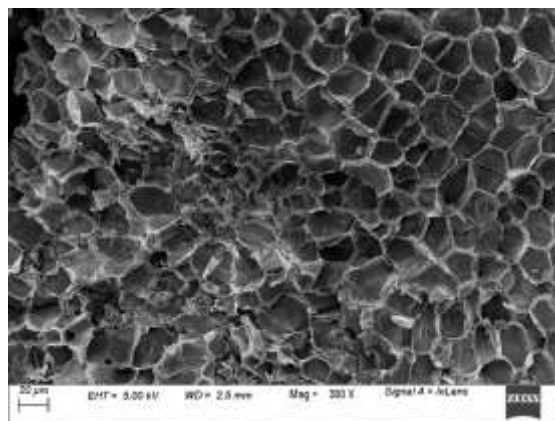


Fig. 2: SEM image of AGT after chromium adsorption

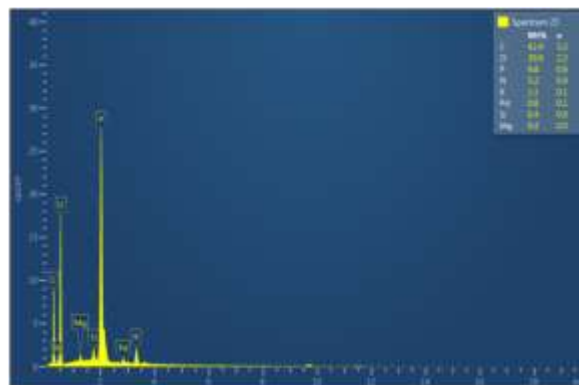


Fig. 3: EDAX analysis of AGT before chromium adsorption

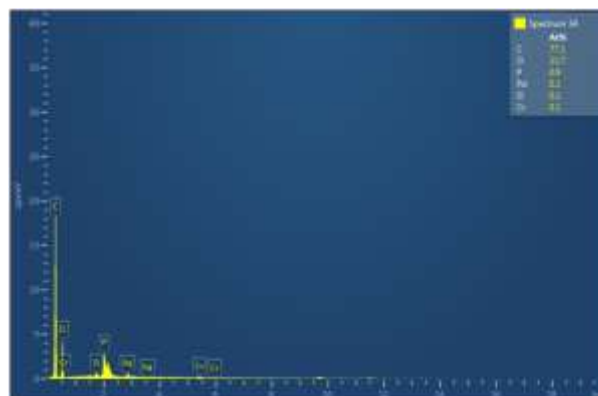


Fig. 4: EDAX analysis of AGT after chromium adsorption

B. Effect of pH

pH of the experimentations were conducted in the range of 2–10 by keeping the other factors constant (time 180 min,

agitation rate of 250 rpm, amount of adsorbents 2 g, with Cr(VI) concentration at 20 ppm and temperature of 303 K) as shown in Fig. 5. With the increase in pH, reduction of chromium is decreased [6]. At low pH, negatively charged chromium compound (CrO_4^{2-} and HCrO_7^{2-}) is expected to easily attract the protonated charge on the surfaces of the adsorbents. But at higher pH, the electrostatic attraction decreases due to the decrease in the positive charges on the adsorbent surfaces. At pH of 2 the highest percentage removal of the ion was obtained with an efficiency of 85.27%. Hence, optimum pH for Cr (VI) removal by AGT was achieved at pH of 2.

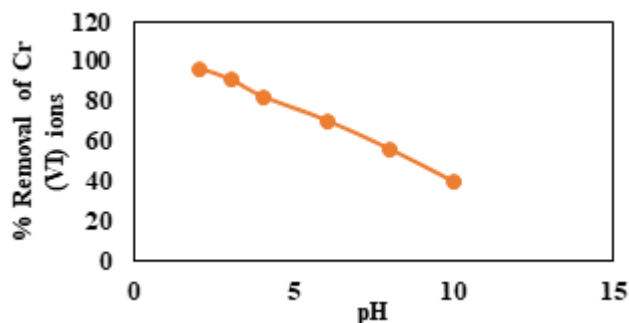


Fig.5:Plot of pH effect on Chromium adsorption

C. Effect of adsorbent dosage

The changes in Cr (VI) ion removal percentage with the metal uptake and the adsorbent dose are shown in Fig. 6. The removal percentage of Cr (VI) ions increases from 54.19 and 85.27% and the uptake of metal decreases from 5.419 and 1.42 mg/g with the increasing dosage from 1 - 6g/L at 303 K. The reduction in the size of the adsorbent increases the surface area for the metal uptake thereby increasing the availability of active sites. No significant increase in the total chromium removal was seen above the dosage of 4 g/L. Thus, optimum dose for Chromium adsorption was obtained at 4g/L for the adsorbent AGT

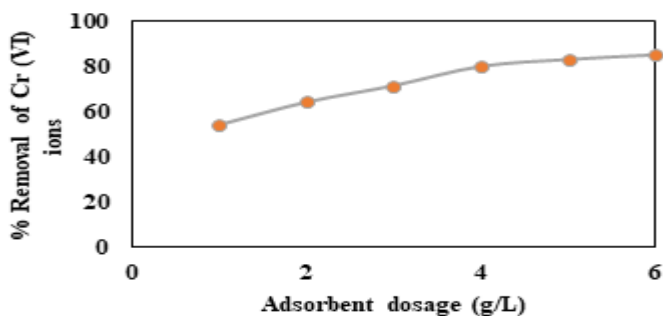


Fig.6:Plot of dosage effect on chromium adsorption

D. Effect of contact time

The removal kinetics was studied by varying the time of contact at optimum pH and dosage of 2 and 4 g/L respectively as shown in Fig. 7. The Cr (VI) removal by AGT increases with time and attains maximum at about 120 min, thereafter it remained almost constant. At the first 40 mins, almost 30% to 70% removal of total chromium was achieved. Later, the removal efficiency reaches to 86% achieving equilibrium. It can be noted that after the saturation of the binding sites, adsorption process stopped even with the increase on adsorbent dosage. The plots are smooth and continuous suggesting the possible monolayer adsorption on the surfaces of the adsorbent AGT.

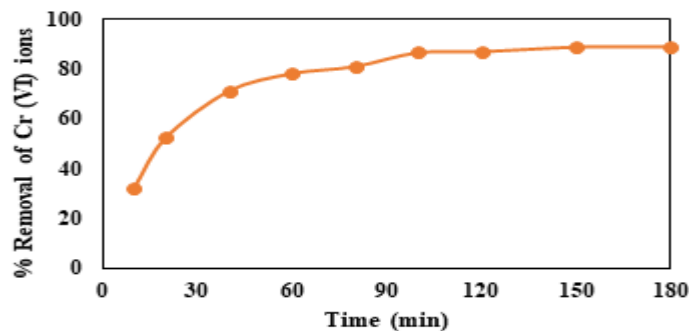


Fig.7:Plot of effect of time on AGT adsorbent

E. Adsorption kinetics

The adsorption kinetics of chromium ions with AGT was studied using intra - particle diffusion, pseudo first order and second order kinetics [7].

$$q_t = K_{IPD}t^{1/2} + C \dots \dots \dots (3)$$

$$\log(q_e - q_t) = \log q_e - \frac{K_1 t}{2.303} \dots \dots \dots (4)$$

$$\frac{t}{q_t} = \frac{1}{K_2 q_e^2} + \frac{t}{q_e} \dots \dots \dots (5)$$

Where, q_t (mg/g) is the adsorption at time t (min), q_e (mg/g) is the adsorption capacity at equilibrium, K_{IPD} , K_1 and K_2 are the kinetic rate constants of intra particle diffusion, first order and second order kinetics respectively.

For Intraparticle diffusion, \sqrt{t} vs q_t was plotted in Fig. 8 using Eqn. 3. The values of intraparticle diffusion constant K_{IPD} (0.171) and boundary layer thickness C (0.99) for the adsorbent were obtained from the slope and intercept of the graph plotted. The adsorption data plotted shows poor linearity for intra particle diffusion model. The R^2 (0.83) value of the adsorbent is not close to unity, conforming that adsorption process do not follow the intra particle diffusion model.

Fig. 9 represents the Pseudo-first-order kinetic plot for time vs $\log(q_e - q_t)$ for Cr (VI) ions removal by AGT. According to the data interpretation, it can be seen adsorption kinetics do not follow first order model, since the R^2 value is not very close to 1. The pseudo-second-order kinetics for adsorption of chromium by AGT is shown in Fig.10. It can be seen from Table 1 that q_{ecal} and q_{eexp} are almost the same with R^2 values of 0.99 each (close to unity) for the adsorbent AGT. Therefore, the second-order kinetic model was found best fitted with the experimental data for hexavalent chromium removal by AGT adsorbent.

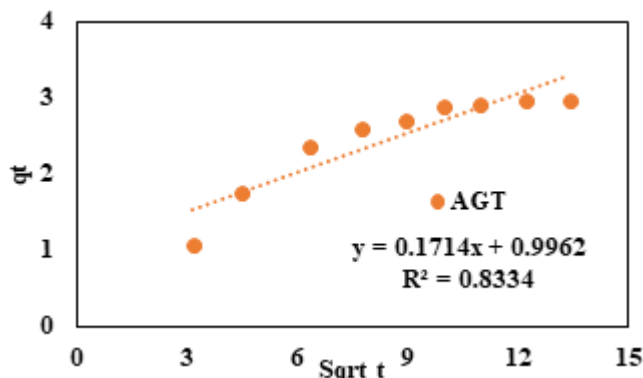


Fig.8: Intra Particle Diffusion model for chromium ions adsorption onto AGT

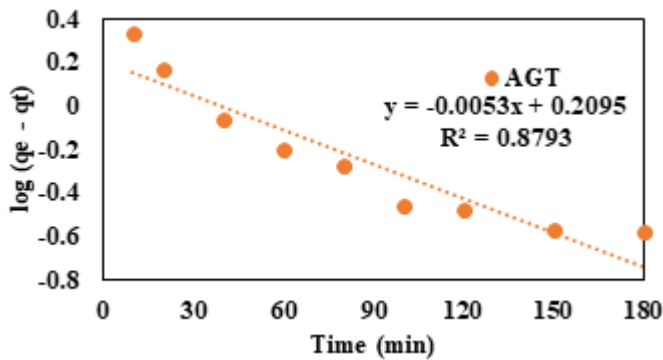


Fig.9: Pseudo first order kinetic model for chromium ions adsorption onto AGT

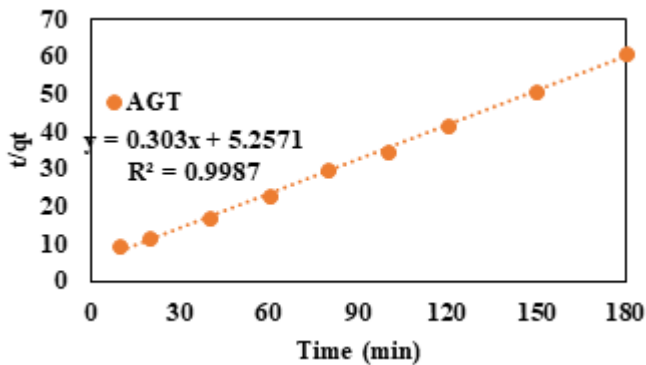


Fig.10: Pseudo second order kinetic model for chromium ions adsorption onto AGT

Table 1: Parameters for different kinetic models

Intra - particle diffusion	K_{IPD}	C	R^2	χ^2
		0.171	0.99	0.833
Pseudo first order	K_1	R^2	q_e (cal)	χ^2
		0.002	0.93	2.896
Pseudo second order	K_2	R^2	q_e (cal)	χ^2
		0.303	0.99	3.3

F. Adsorption Isotherms

The adsorption isotherms describes the effect of concentrations of the solutions on adsorption capacities of chromium ions and the interactions of the adsorbates on the adsorbents [8]. The adsorbent AGT is equilibrated with chromium ions at different concentrations with pH of 2, dosage 4 g/L and 120 min of contact time. The adsorption isotherm models, Langmuir and Freundlich were used to describe the adsorption of chromium ions on AGT adsorbent.

$$\frac{C_e}{q_e} = \frac{C_e}{q_m} + \frac{1}{K_L q_m} \dots \dots \dots (6)$$

$$\ln q_e = \ln K_F + \frac{1}{n} \ln C_e \dots \dots \dots (7)$$

Where, q_m and K_L are maximum adsorption capacity and Langmuir constant respectively. K_F and n are the Freundlich adsorption capacity and heterogeneity factor respectively.

Langmuir adsorption isotherm was obtained by plotting C_e vs C_e/q_e as shown in Fig. 11. R^2 value obtained from the plot shows poor linearity for Langmuir isotherm. The equations with correlation coefficients (R^2) are shown in Table 4.7. It can be concluded that the adsorption isotherm for AGT adsorbent do not follow Langmuir's isotherm model. Whereas, the Freundlich isotherm data for the adsorption of Cr (VI) on AGT

plotted in Figure 12, shows good linearity for Freundlich Isotherm. The equations with correlation coefficients (R^2), K_F , Freundlich adsorption capacity an indicator of the process, whether favourable or not and n , the adsorption intensity which represents the fitness of the model, were obtained from the slope and intercept of the plot and listed are in Table 2. Linearity of the relationship indicates strong binding of Cr (VI) to the adsorbent (Ahmed et al., 2011). The slope of isotherm was found to be 1.0598 fulfilling the condition of $n > 1$ for favourable adsorption. The values of R^2 obtained represent good fitness of the model for Cr (VI) adsorption.

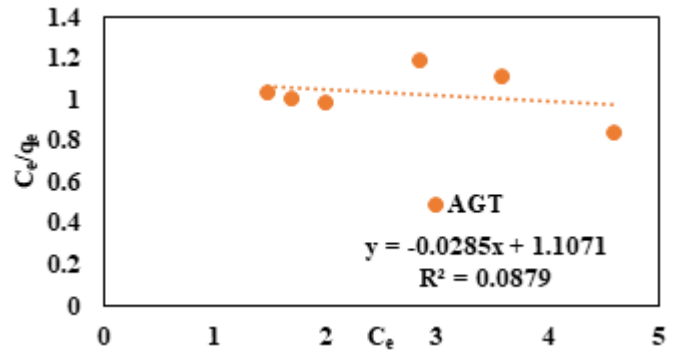


Fig.11: Langmuir isotherm model for chromium ions adsorption onto AGT

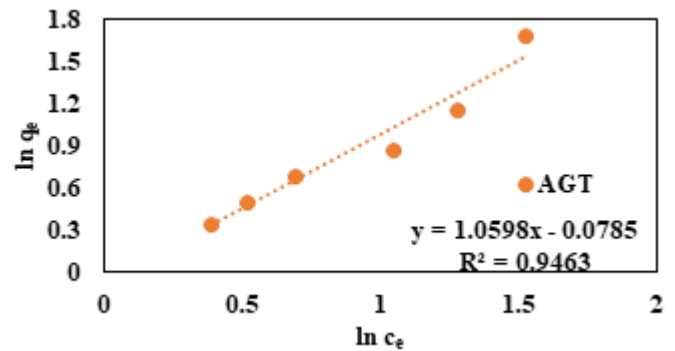


Fig.12: Freundlich isotherm model for chromium ions adsorption onto AGT

Table 2: Parameters for different isotherm models

Langmuir Isotherm	K_L (L/mg)	q_m (mg/g)	R^2
		1.38	5.419
Freundlich Isotherm	K_F (mg/g)	n	R^2
	3.522	1.259	0.946

G. Adsorption thermodynamics

The effects of temperature on the adsorption capacity of chromium solution was investigated at different temperatures (298, 308, 318 and 333K) at pH of 2 and contact time of 120 min. the thermodynamic parameters for chromium ions adsorption on AGT adsorbent was estimated using the equations [6]:

$$\ln K = \frac{\Delta S}{R} - \frac{\Delta H}{RT} \dots \dots \dots (8)$$

$$\Delta G = -RT \ln K \dots \dots \dots (9)$$

$$K = \frac{q_e}{C_e} \dots \dots \dots (10)$$

Where, R is the universal gas constant (8.314 J mol), T is the temperature (K), K is the thermodynamic equilibrium constant.

The enthalpy (ΔH) and entropy (ΔS) were calculated from the slope and intercept of the plot of $\ln K$ vs $1/T$ as shown in Fig. 13, and the thermodynamic parameters for the adsorbent AGT is given in Table 3. The negative value of ΔG and ΔH indicates that the adsorption reaction was exothermic and that the adsorption of chromium ions on AGT adsorbent were spontaneous all throughout the process.

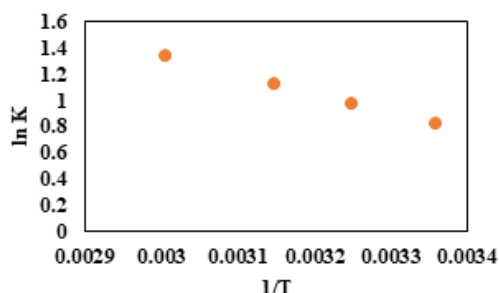


Fig.13: Thermodynamic parameter plot for chromium ions adsorption onto AGT

Table 3: Thermodynamic parameters of Chromium ions on AGT adsorbent

T (K)	ΔG (KJ/mol)	ΔS	ΔH	R^2
298	-2.450	0.047	-12.22	0.99
308	-2.907			
318	-3.577			
333	-3.745			

IV. CONCLUSION

Giant taro were synthesized in acidic medium using H_3PO_4 to get activated Giant taro (AGT). On characterization, the surface was found to be porous, with large surface areas and pore diameters. Optimum pH for removal of Cr (VI) by AGT was observed at pH of 2 with maximum removal of 5.419 mg/g by electrostatic attraction between the protonated amines (NH_3^+) on the AGT surfaces and chromate ions ($HCrO_4^-$). At acidic pH, maximum chromium reduction of 20% was seen. The evaluated data kinetic data clearly implies that pseudo second order model fits better as compared to pseudo first order model with least Chi square (χ^2) value of 0.08. And the equilibrium adsorption data fitted best with the Freundlich isotherms with a correlation coefficient of 0.99.

REFERENCES

- [1] Bhatnagar A., Mika S. and Anna W. (2015) "Agricultural waste peels as versatile biomass for water purification – A review", *Chem.Engg. Jr.* 270, 244-271.
- [2] Haddad M. E. (2018). "Removal of Basic Fuchsin dye from water using mussel shell biomass waste as an adsorbent: Equilibrium, kinetics, and thermodynamics", *Jr. of Taibah Univ. for Sc.*, 10, 245-254.
- [3] Abbas M. (2021). "Mass Transfer Processes in the Adsorption of Lead (Pb^{2+}) by Apricot Stone Activated Carbon (ASAC): Isotherms Modeling and Thermodynamic Study", *Protection of Metals and Physical Chem. of Surfaces, Protection of Metals and Physical Chem.of Surfaces*, 57(4), 687-698.
- [4] Reddy, D., Kumar H., and Lee S. M. (2013). "Three-dimensional porous spinel ferrite as an adsorbent for Pb

(II) removal from aqueous solutions", *Industrial & Engg. Chem. Research*, 52(45), 15789-15800.

- [5] Kumar, P. A. and Ray M. (2007). "Hexavalent chromium removal from wastewater using aniline formaldehyde condensate coated silica gel", *Jr. of Hazard. Mat.* 5(8).
- [6] Mathew B. B., Jaishankar M, Biju V. G. and Beeregowda K. N., (2016) "Role of Bioadsorbents in reducing Toxic Metals", *Jr. of Toxicol.*, 5, 15-21.
- [7] S. Sujatha and R. S. Mohan, "A critical review of Cr(VI) ion effect on mankind and its amputation through adsorption by activated carbon", *Materials today proceedings*, Vol. 37(2), pp. 1158-1162, April 2021.
- [8] S. Sangeeta and P. A. Kumar, "Efficacy of bio-carbon mediated chromium absorption from contaminated groundwater: A kinetic approach", *Journal of Indian Chemical Society*, vol. 10(b), pp. 1-4, October, 2020.